

## Evidence for Roughness Driven 90° Coupling in Fe<sub>3</sub>O<sub>4</sub>/NiO/Fe<sub>3</sub>O<sub>4</sub> Trilayers

P. A. A. van der Heijden,\* C. H. W. Swüste, and W. J. M. de Jonge

*Department of Physics, Interuniversity Research Institute COBRA, Eindhoven University of Technology,  
5600 MB Eindhoven, The Netherlands*

J. M. Gaines, J. T. W. M. van Eemeren, and K. M. Schep

*Philips Research Laboratories, Prof. Holstlaan 4, 5656 AA Eindhoven, The Netherlands*

(Received 18 September 1998)

The magnetic interlayer coupling of Fe<sub>3</sub>O<sub>4</sub> across NiO is studied using Fe<sub>3</sub>O<sub>4</sub>/NiO/Fe<sub>3</sub>O<sub>4</sub> trilayers epitaxially grown on (001) MgO substrates. For NiO thicknesses between 0.7 and 5 nm, the magnetic moments of the two Fe<sub>3</sub>O<sub>4</sub> layers are directed perpendicularly with respect to each other. The 90° coupling strength is determined to be  $0.35 \pm 0.08$  mJ/m<sup>2</sup> for a 1.4-nm-thick NiO spacer. The 90° coupling can be understood from the effect of an antiferromagnetic spacer in the presence of interface roughness. [S0031-9007(99)08387-8]

PACS numbers: 75.70.Cn, 75.50.Ss, 75.60.Lr

Since the first observation of coupling between magnetic layers over an ultrathin metallic spacer, this issue has fused an enormous amount of experimental and theoretical activity. By now the (oscillatory) interaction mediated by a metallic spacer is fairly well understood in terms of an RKKY-related electron optic interference model [1]. This emphasizes the crucial role of the Fermi surface of the carriers in the spacer layer. For insulating spacers the coupling is less clear. The RKKY-like contributions to the interlayer coupling are absent and, as was theoretically shown, an exponential decreasing interaction related to electron tunneling may be anticipated in the limit of ultrathin spacer layers [2,3]. In the case of an antiferromagnetic (AFM) insulating spacer, one may anticipate an interlayer coupling contribution originating from the propagating nearest AFM exchange coupling in the spacer, which one may imagine to result in an oscillating interlayer coupling. However, so far, such behavior has not been reported for insulating spacer layers.

In this Letter, we report on the interlayer coupling in Fe<sub>3</sub>O<sub>4</sub>/NiO/Fe<sub>3</sub>O<sub>4</sub> trilayers. We will show that for the insulating and AFM NiO spacers in the range of 0.7–5 nm, a perpendicular arrangement of the magnetic moments of the two Fe<sub>3</sub>O<sub>4</sub> layers is observed. Above 5 nm, however, a gradual alignment of the magnetic moments takes place. The observed 90° coupling can be understood in terms of a mechanism where the 90° coupling is driven by the combined effect of a propagating nearest neighbor coupling in the AFM-spacer and roughness at the interface.

Fe<sub>3</sub>O<sub>4</sub>/NiO/Fe<sub>3</sub>O<sub>4</sub> trilayers were epitaxially grown on (001) MgO substrates at 500 K by molecular beam epitaxy (MBE). The Fe<sub>3</sub>O<sub>4</sub> and NiO layers were deposited by means of e-gun evaporation from Fe and Ni targets, respectively, in an ambient O<sub>2</sub> atmosphere of  $2.8 \times 10^{-5}$  mbar. Two wedge-type samples were grown composed of 20 nm Fe<sub>3</sub>O<sub>4</sub>/0–2 nm NiO/20 nm Fe<sub>3</sub>O<sub>4</sub> and 25 nm Fe<sub>3</sub>O<sub>4</sub>/0–9 nm NiO/25 nm Fe<sub>3</sub>O<sub>4</sub>. The local

magneto-optical longitudinal Kerr effect (MOKE) was used to characterize the magnetic behavior as a function of the NiO layer thickness. Since the penetration depth is far more than the thickness of the present system, the total magnetization is observed [4].

The hysteresis loops shown in Fig. 1 on a 20 nm Fe<sub>3</sub>O<sub>4</sub>/0.4 nm NiO/20 nm Fe<sub>3</sub>O<sub>4</sub> trilayer are representative for the magnetic behavior observed for NiO spacers in the range of 0–0.7 nm. The longitudinal MOKE experiments are performed in two geometries in which the in-plane magnetization is measured either parallel or perpendicular to the in-plane applied field as sketched in the inset of Fig. 1. The hysteresis loops in Fig. 1 monitoring the magnetization parallel to an applied field along a [110] direction show a remanent magnetization of almost 100% while the magnetization perpendicular to that axis is practically zero. After applying a field along [100] a remanent magnetization of 70% along [100] as well as perpendicular to [100] is observed. The overall magnetic behavior and the observation of a fourfold symmetry (not shown) is characteristic for a single magnetic domain with easy ⟨110⟩ and hard ⟨100⟩ in-plane magnetization axes. Such magnetic behavior is expected for a single (001) Fe<sub>3</sub>O<sub>4</sub> layer with cubic magnetocrystalline anisotropy [5]. Therefore, the magnetic behavior observed below 0.7 nm NiO can be understood by assuming no coupling at all or, more likely, a ferromagnetic (FM) coupling between the Fe<sub>3</sub>O<sub>4</sub> layers, which is commonly observed for small spacer thicknesses and arises from ferromagnetic bridges across the thin NiO spacer (“pinholes”) [6].

A completely different hysteresis behavior is observed for trilayers with a NiO spacer thickness above 0.7 nm, as shown in Fig. 2. For  $H \parallel [110]$  the parallel remanent magnetization is reduced to  $0.5M_s$  and equals the perpendicular component, while for  $H \parallel [100]$  the zero field parallel magnetization is  $0.7M_s$  and virtually no perpendicular component is observed. Moreover, when compared to the

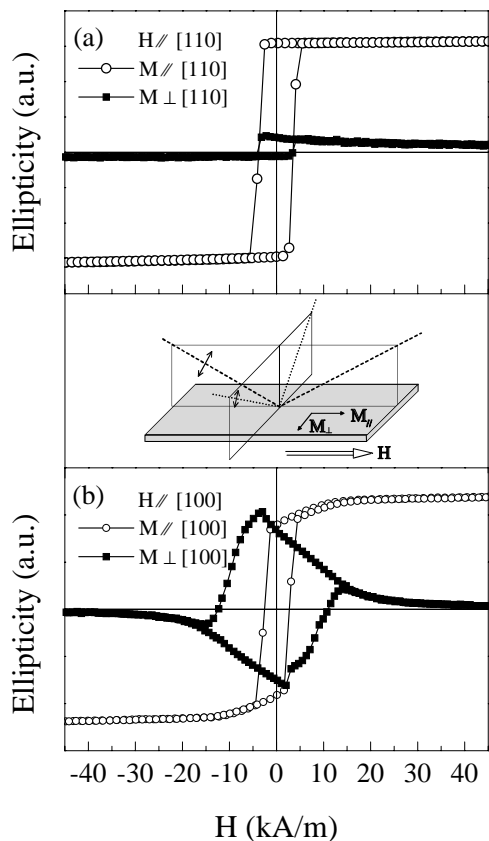


FIG. 1. Longitudinal MOKE measurements on a 20 nm  $\text{Fe}_3\text{O}_4/0.4$  nm NiO/20 nm  $\text{Fe}_3\text{O}_4$  trilayer with the field applied along [110] (a) and [100] (b). The ellipticity is a measure of the magnetization parallel and perpendicular to the applied field. The two MOKE geometries applied to obtain the two components of the magnetization are shown in the inset. The (small) contribution of  $M_{\perp}$  in (a) is most probably caused by a small misorientation.

results for the thinner NiO spacers, a strong increase is observed of the saturation fields. Qualitatively this behavior can be understood if (at zero field) the magnetizations  $\mathbf{M}_1$  and  $\mathbf{M}_2$  of the two layers are oriented perpendicular to each other along the mutually perpendicular easy [110] and  $[-110]$  directions. Saturation by application of a field requires the alignment of  $\mathbf{M}_1$  and  $\mathbf{M}_2$  and would therefore also explain (at least qualitatively) the increase of the saturation field.

To investigate this apparent  $90^\circ$  coupling more quantitatively, we have performed in-plane hysteresis loop calculations for two  $\text{Fe}_3\text{O}_4$  layers with thicknesses  $t_1$  and  $t_2$  (both 20 nm) with a bulk value for the magnetization ( $M_s = 496$  kA/m) [7] and cubic magnetocrystalline anisotropy  $K_1$  ( $-9$  kJ/m $^3$ ) [5] and assuming a (phenomenological)  $90^\circ$  interlayer coupling,  $J_2$ . The in-plane angular dependence of the energy per unit area is given by

$$E = -\mu_0 M_s t_1 H \cos(\phi_1 - \theta) - \mu_0 M_s t_2 H \cos(\phi_2 - \theta) + K_1 t_1 \cos^2 \phi_1 \sin^2 \phi_1 + K_1 t_2 \cos^2 \phi_2 \sin^2 \phi_2 + J_2 \cos^2(\phi_1 - \phi_2), \quad (1)$$

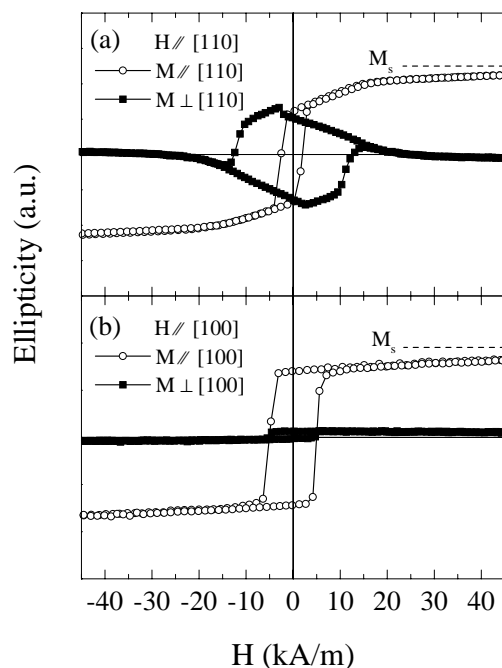


FIG. 2. Hysteresis loops of 20 nm  $\text{Fe}_3\text{O}_4/1.4$  nm NiO/20 nm trilayer obtained by longitudinal MOKE experiments. Again the magnetization parallel and perpendicular to the applied field is monitored by using two different MOKE geometries, similar to the case with a 0.7 nm NiO spacer.

in which  $\phi_1$ ,  $\phi_2$ , and  $\theta$  are the angles of the magnetic moments,  $\mathbf{M}_1$  and  $\mathbf{M}_2$ , and the applied field, respectively, with respect to [100]. In the calculations, the energy is locally minimized as a function of  $\phi_1$  and  $\phi_2$ .

Figure 3 shows the calculated hysteresis loops for the field applied along [110] and [100]. For  $J_2 = 0.35 \pm 0.08$  mJ/m $^2$ , the calculated hysteresis loop behavior is similar to the experimentally observed hysteresis loop behavior, specifically regarding the kink position around 20 kA/m and the estimated saturation. It is interesting to note that applying a field along [110], that is along  $\mathbf{M}_1$  and perpendicular to  $\mathbf{M}_2$ , results initially in a predominant rotation of the almost rigid  $90^\circ$  unit of the magnetic moments to a symmetrical position of  $\mathbf{M}_1$  and  $\mathbf{M}_2$  around the field. At higher fields  $\mathbf{M}_1$  and  $\mathbf{M}_2$  gradually align along the applied field. This change in the magnetic process is reflected by the kink in the calculated hysteresis loop of Fig. 3, which is also observed experimentally; see Fig. 2.

Several coupling mechanisms can give rise to  $90^\circ$  coupling between two magnetic layers. However, most of these coupling mechanisms are unlikely for the present case of two magnetite layers separated by a NiO spacer. The “RKKY-like” coupling mechanisms can be excluded for the present *insulating* NiO layer. Also interlayer coupling arising from spin-polarized tunneling across an insulator is unlikely for these interlayer thicknesses. A  $90^\circ$  coupling arising from magnetostatic coupling between the two magnetite layers due to uncorrelated interface roughness [8] can be excluded on the basis of a previous study [6].

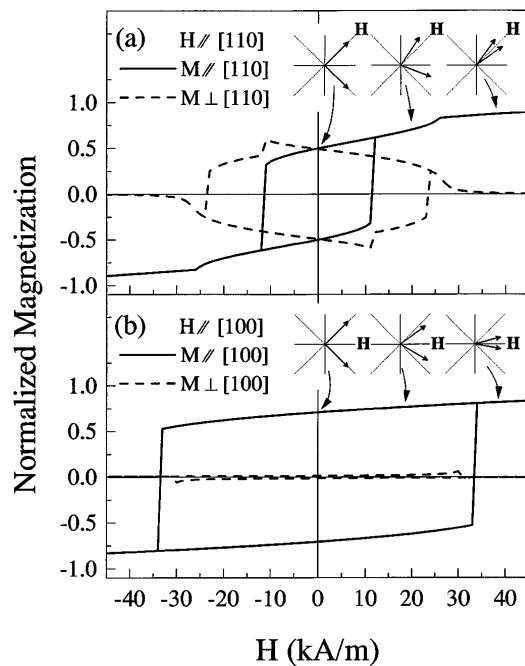


FIG. 3. Calculations of the hysteresis loop behavior for two magnetic layers with an in-plane cubic anisotropy and mutual  $90^\circ$  coupled for the field applied along  $[110]$  (a) and  $[100]$  (b). The schematic drawings show the configurations of the magnetic moments (represented by the arrows) at different positions of the hysteresis loop.

The most likely mechanism for the observed  $90^\circ$  coupling is that suggested by Slonczewski [9]. This model has also been employed to explain the giant near- $90^\circ$  coupling observed recently across metallic metastable body-centered tetragonal (bct) Mn spacers [10]. In this model, the coupling of two ferromagnetic layers across an AFM spacer is mediated by the short range Heisenberg exchange coupling. For perfectly flat interfaces and an uncompensated AFM interface this results in either ferro- or antiferromagnetic coupling between the two FM layers, depending on the number of AFM planes. Interface roughness results in lateral variations in the number (odd or even) of intermediate AFM planes, and thereby in a competition between ferro- and antiferromagnetic coupling between the two FM layers. The resulting overall interaction between the FM layers can be calculated when the interaction between the spins in adjacent areas of the AFM spacer can be neglected. In the limit of large thickness and random roughness, the mean coupling  $W$  has the form

$$W = 2C(\phi_1 - \phi_2 - \pi/2)^2, \quad (2)$$

in which  $C$  indicates the strength of the coupling. Equation (2) gives rise to an effective  $90^\circ$  coupling between the magnetizations of the FM layers [9], and therefore relates to the phenomenological  $J_2$  in Eq. (1). Physically, the  $90^\circ$  coupling results from a  $90^\circ$  rotation of the sublattice spin directions of the AFM spacer going from one FM/AFM interface to the other as is sketched in Fig 4(b).

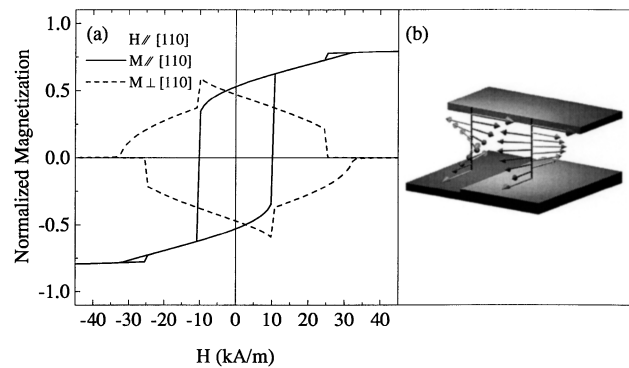


FIG. 4. Calculated hysteresis loops for a 20 nm  $\text{Fe}_3\text{O}_4/1.2$  nm  $\text{NiO}/20$  nm  $\text{Fe}_3\text{O}_4$  trilayer on the basis of the extended Slonczewski model (a). (b) shows a schematic drawing of the spin configuration for a perpendicular orientation of the spins of the two ferromagnetic layers in the case of  $n = 13$  and  $n - 1 = 12$  intermediate AFM planes.

The model is applicable if the scale of the lateral interface fluctuations is sufficiently large, which is the case for the present samples. STM measurements show large atomically flat terraces extending over several tens of nanometers for an  $\text{Fe}_3\text{O}_4$  layer grown on  $(001)$   $\text{MgO}$  [11]. The requirement of an uncompensated AFM-interface plane seems at first sight not to be fulfilled, since  $(001)$   $\text{NiO}$  has a compensated interface. However, the magnetic lattice parameter in a  $(001)$   $\text{Fe}_3\text{O}_4$  plane [12] is almost exactly twice (mismatch only 0.5%) that of  $\text{NiO}$ . As a consequence, in an epitaxially grown system the surface spins of the  $\text{Fe}_3\text{O}_4$ , in a first approximation, interact only with one of the two uncompensated sublattices of the  $(001)$   $\text{NiO}$  interface plane. This model has also been suggested earlier, to explain the sizable interface interaction between  $\text{Fe}_3\text{O}_4$  and  $\text{CoO}$  [13].

In Slonczewski's model only nearest-neighbor Heisenberg exchange in the spacer is assumed, which results in a constant angle difference between adjacent AFM spins throughout the AFM spacer. In order to obtain a more realistic description, we have extended the model with the anisotropy of the AFM spacer. Such an inclusion of the AFM anisotropy is expected to result in a nonuniform spin rotation in the AFM spacer and a significant change of the coupling energy. For these calculations, the  $\text{Fe}_3\text{O}_4$  layers are again modeled by a single magnetic domain with appropriate Zeeman and anisotropy terms [see Eq. (1)]. For  $\text{NiO}$ , the bulk spin structure is used and the exchange coupling constant  $J_{\text{AFM}}$  between adjacent spins is taken to be 130 K as derived from  $T_N$ . Since the experiments show a fourfold symmetry of the magnetic behavior independent of the presence or absence of the  $90^\circ$  coupling, the in-plane anisotropy of  $\text{NiO}$  is modeled by a cubic anisotropy ( $K_{\text{AFM}}$  of  $-0.5$   $\text{MJ}/\text{m}^3$ ) with the same easy magnetization axes as in  $\text{Fe}_3\text{O}_4$ . Numerically,  $K_{\text{AFM}}$  equals the bulk uniaxial anisotropy constant of  $\text{NiO}$  [14]. The  $\text{NiO}$  spacer is represented by two rows with  $n$  and  $n - 1$  intermediate AFM planes between the  $\text{Fe}_3\text{O}_4$  layers, as schematically

sketched in Fig. 4(b). The rows of AFM spins are coupled at the interfaces to the  $\text{Fe}_3\text{O}_4$  layer ( $J_{\text{interface}} = 130$  K), but are laterally decoupled. Since the value of  $J_{\text{interface}}$  appears not to be a very sensitive parameter in the calculations, it is taken to be the same as in NiO.

The hysteresis loops can be obtained by micromagnetic (mean-field) numerical calculations. Figure 4(a) shows a hysteresis loop calculated for the field applied along  $[110]$ . The obtained hysteresis loop behavior is similar to that shown in Fig. 3 including the occurrence of the kink at about 20 kA/m and the remanent magnetization of  $0.5M_s$ . In agreement with Slonczewski, saturation is approached asymptotically but at rather high fields, which is not understood at the moment. Nevertheless, the results show that the observed  $90^\circ$  coupling can be reproduced by the extended Slonczewski model. It has to be noted that the introduction of  $K_{\text{AFM}}$  is vital to the results. Without the anisotropy an unrealistic  $J_{\text{AFM}}$  of 13 K has to be used to obtain a similar agreement.

The dependence of the interlayer coupling on the NiO layer thickness was studied by local longitudinal MOKE experiments as a function of the position on wedge type samples. The remanent magnetization along  $[110]$  for NiO thickness in the range of 0.7–5 nm is fairly constant, in agreement with the  $90^\circ$  coupling observed in that range and documented above for the NiO spacer of 1.4 nm. Above 5 nm, however, a gradual increase of the remanence is observed, indicating a gradual alignment of the moments of the two  $\text{Fe}_3\text{O}_4$  layers. This behavior can be understood since a perpendicular arrangement of  $\mathbf{M}_1$  and  $\mathbf{M}_2$  at zero field can be obtained only if the  $90^\circ$  coupling is larger than the in-plane magnetocrystalline anisotropy barrier, i.e.,  $J_2 > t_i K_1/2$  ( $= 0.09$  mJ/m<sup>2</sup>). As we have determined that the microscopic origin of the  $90^\circ$  coupling can be described by Slonczewski's model, the phenomenological coupling constant  $J_2$  is related to  $C$  in Eq. (2). According to Slonczewski's model,  $C$  decreases proportional to the reciprocal AFM spacer thickness. Using the fit value for  $J_2$  of 0.35 mJ/m<sup>2</sup> obtained for a NiO spacer of 1.4 nm, this implies that  $J_2$  can be expected to be smaller than  $t_i K_1/2$  for NiO spacer thicknesses above 5.4 nm. Consequently, the perpendicular arrangement of the ferromagnetic moments at zero field cannot be established for NiO thicknesses above 5.4 nm, and an increase of the remanent magnetization along  $[110]$  can be expected, which agrees with the experimental observation. The same mechanism might also be responsible for the vanishing coupling for thick metallic bct Mn as observed before [10].

Concluding, we have shown that in  $\text{Fe}_3\text{O}_4/\text{NiO}/\text{Fe}_3\text{O}_4$  the insulating and AFM interlayer can sustain a  $90^\circ$  cou-

pling, driven by a short range nearest-neighbor exchange, which propagates through the spacer and lateral interface roughness. The anisotropy of the magnetic layer as well as of the AFM spacer play an important part yielding a vanishing coupling at larger thickness. The  $90^\circ$  coupling at room temperature may present interesting options for magnetoengineering and applications.

We would like to thank L.F. Feiner, P.J. van der Zaag, A.A. Smits, and G.J. Strijkers for carefully reading the manuscript and valuable discussions. Part of this work was supported by the Dutch Technology Foundation (STW) and the EU-ESPRIT project on Novel Magnetic Nanodevices of artificially layered Materials (NM)<sup>2</sup>.

---

\*Present address: AMC, 75 Robin Hill Road, Goleta, CA 93117.

- [1] P. Bruno, *Europhys. Lett.* **23**, 615 (1993).
- [2] J.C. Slonczewski, *Phys. Rev. B* **39**, 6995 (1989).
- [3] P. Bruno, *Phys. Rev. B* **49**, 13 231 (1994).
- [4] W.F.J. Fontijn, R.M. Wolf, R. Metselaar, and P.J. van der Zaag, *Thin Solid Films* **292**, 270 (1997).
- [5] P.A.A. van der Heijden, M.G. van Opstal, C.H.W. Swüste, P.H.J. Bloemen, J.M. Gaines, and W.J.M. de Jonge, *J. Magn. Magn. Mater.* **182**, 71 (1998).
- [6] P.A.A. van der Heijden, P.J.H. Bloemen, J.M. Metselaar, R.M. Wolf, J.M. Gaines, J.T.W.M. van Eemeren, P.J. van der Zaag, and W.J.M. de Jonge, *Phys. Rev. B* **55**, 11 569 (1997).
- [7] V.A.M. Brabers, in *Handbook of Magnetic Materials*, edited by K.H.J. Buschow (Elsevier Science, Amsterdam, 1995), Vol. 8, Chap. 3.
- [8] S. Demokritov, E. Tsybmal, P. Grünberg, W. Zinn, and I.K. Schuller, *Phys. Rev. B* **49**, 720 (1994).
- [9] J.C. Slonczewski, *J. Magn. Magn. Mater.* **150**, 13 (1995).
- [10] M.E. Filipkowski, J.J. Krebs, G.A. Prinz, and C.J. Gutierrez, *Phys. Rev. Lett.* **75**, 1847 (1995).
- [11] J.M. Gaines, P.J.H. Bloemen, J.T. Kohlhepp, C.W.T. Bulle-Lieuwma, R.M. Wolf, A. Reinders, R.M. Jungblut, P.A.A. van der Heijden, J.T.W.M. van Eemeren, J. aan de Stegge, and W.J.M. de Jonge, *Surf. Sci.* **373**, 85 (1997).
- [12] J.A. Borchers, R.W. Erwin, S.D. Berry, D.M. Lind, J.F. Ankner, E. Lochner, K.A. Shaw, and D. Hilton, *Phys. Rev. B* **51**, 8276 (1995).
- [13] P.J. van der Zaag, A.R. Ball, L.F. Feiner, R.M. Wolf, and P.A.A. van der Heijden, *J. Appl. Phys.* **79**, 5103 (1996).
- [14] A.J. Sievers III and M. Tinkham, *Phys. Rev.* **129**, 1566 (1963).